The Structure of a Model Pulmonary Surfactant as Revealed by Scanning Force Microscopy

A. von Nahmen,* M. Schenk,# M. Sieber,* and M. Amrein#
*Institut für Biochemie and #Institut für Medizinische Physik und Biophysik, Westfälische Wilhelms-Universität, D-48149 Münster, Germany

ABSTRACT The structures formed by a pulmonary surfactant model system of dipalmitoylphosphatidylcholine (DPPC), dipalmitoylphosphatidylglycerol (DPPG), and recombinant surfactant-associated protein C (SP-C) were studied using scanning force microscopy (SFM) on Langmuir-Blodgett films. The films appeared to be phase separated, in agreement with earlier investigations by fluorescence light microscopy. There were smooth polygonal patches of mostly lipid, surrounded by a corrugated rim rich in SP-C. When the films were compressed beyond the equilibrium surface pressure, the protein-rich phase mediated the formation of layered protrusions. The height of these multilamellar structures embodied equidistant steps slightly higher than a DPPC double layer in the gel phase. At the air-water interface too, a high compressibility at low surface tension was indicative of the exclusion of matter. The exclusion process proved to be fully reversible. The present study demonstrates that some of the matter of the model pulmonary surfactant can move in and out of the active monolayer. The SFM images revealed a lipid-protein complex that was responsible for the reversible exclusion of double-layer structures. This mechanism may be important in the natural system too, to keep the surface tension of the alveolar air/water interface constantly low over the range of area encountered upon breathing.

INTRODUCTION

The surface of the alveolar epithelium of the lungs is highly solvated. This results in the formation of an aqueous interface to the air. The surface tension of this interface is strongly reduced in all air-breathing vertebrates by a surface-active material known as the pulmonary surfactant. It keeps the surface tension persistently low upon breathing and provides stability to the alveoli of different size (Pattle, 1958; Clements et al., 1958). von Neergaard (1929) was responsible for assigning the retractile force of the lung to the surface tension of the alveoli. Pattle and Clements were the first to demonstrate a substance lining the alveoli of mature lungs with the unique physical properties now associated with the pulmonary surfactant.

The lung surfactant, which is quite similar among diverse species (Harwood, 1987), consists primarily of phospholipids (80–90% of its mass). The neutral phosphatidylcholines represent 80% of the phospholipid content in human surfactant. It is uniquely rich in DPPC. Five to ten percent are negatively charged phosphatidylglycerols (Shelly et al., 1982). In addition, there are at least four distinct surfactant-associated proteins, SP-A, SP-B, SP-C, and SP-D (e.g., Possmayer, 1988; Weaver, 1988; Hawgood, 1989; Johansson et al., 1994a). They play a decisive role as well, even though they amount to less than 10% of the surfactant mass.

In 1958 Clements used a Wilhelmy balance to establish the relationship between the surface tension and the molecular area of the pulmonary surfactant (Clements et al., 1958) at the air-water interface. Since that time, the biophysical properties of surfactant extracted from the lung and reconstituted surfactant have been studied extensively at the air-liquid interface. The methods by which this has been accomplished included using a Langmuir surface balance and modifications thereof (e.g., Goerke and Clements, 1986), a pulsating bubble surfactometer (Enhorning, 1977), and a captive bubble surfactometer (Schürch, 1982). These studies have identified the phospholipids as the primary surface tension-lowering component. DPPC plays a major role in this function (Brown, 1964; Notter et al., 1980). The surfactant monolayer theory (SMT) predicts that a surface tension close to zero, required at end expiration, is attained with monolayers consisting almost exclusively of DPPC (Bangham et al., 1979). These films are thought to form upon compression via a reversible exclusion of the surfactant-associated compounds that would prevent such a low surface tension.

SP-B and SP-C are responsible for many of the properties of the pulmonary surfactant. They promote rapid adsorption of vesicular matter from the hypophase to the monolayer at the air-water interface. They cause the phospholipids to spread to the interface until the equilibrium surface tension is reached (Oosterlaken-Dijksterhuis et al., 1991a,b; Pèrez-Gil et al., 1992b; Wang et al., 1995), and they facilitate the adsorption of new surfactant material from the subphase when they are in the monolayer (Oosterlaken-Dijksterhuis et al., 1991a,b). They also trigger the reversible exclusion of matter from the monolayer once it is compressed beyond the equilibrium surface tension (Post et al., 1995; Taneva and Keough, 1994a,b,c,d).

In the present paper, the structural basis of the exclusion process is studied by SFM on a model surfactant. It consists

Received for publication 15 May 1996 and in final form 9 October 1996.
Address reprint requests to Dr. Matthias Amrein, Institut für Medizinische Physik und Biophysik, Westfalische Wilhelms-Universität, Robert-Koch-Strasse 30, D-48149 Munster, Germany. Tel.: 49-251-83-5107; Fax: 49-251-83-5144; E-mail: amrein@uni-muenster.de.

0006-3495/97/01/463/07 $2.00

of DPPC, DPPG, and dipalmitoylated pulmonary surfactant protein C (SP-Cpp). These components are kept close to the natural proportions. SP-Cpp is a small amphipathic polypeptide with a molecular mass of 4 kDa. The carboxy terminal two-thirds of the 33–35 amino acid residues (depending on the species), mainly valine and leucine, are ordered in a highly hydrophobic α-helix (Johansson et al., 1994b). The flexibly disordered amino terminal headgroup includes two palmitoylcysteinyls (Curstedt et al., 1990) and a positively charged arginine and lysine (Qanbar and Possmayer, 1995).

In fluorescence light microscopy, mixed phospholipid/SP-C monolayers appear to be phase separated (Pèrez-Gil et al., 1992a). In the pressure-area diagram measured with a film balance, the "squeeze-out" process becomes evident from a prominent plateau (i.e., a region of high compressibility) near the equilibrium surface pressure of the film (Π = 50 mN/m). Previous investigations (Post et al., 1995; Taneva and Keough, 1994a,c,d) have demonstrated on the basis of surface balance studies that the material removed upon compression remains associated with the monolayer and readily reinserts upon decompression without a loss of material. This surface-associated "reservoir" has also been observed in natural surfactant systems. Tchoreloff et al. (1991) and Schürch et al. (1995) provided structural evidence of such a "reservoir" by means of electron microscopy of Langmuir-Blodgett films of lung surfactant extract and of thin sections of rabbit lungs (fixed by vascular perfusion), respectively. Hence the biophysical properties of the mixed phospholipid/SP-C monolayer mimic the behavior of natural surfactant. This is certainly relevant in exogenous replacement therapy in premature babies who suffer from respiratory distress syndrome (RDS).

The SFM has become an important technique for investigating the organization of thin organic films. We used a partially home-built set-up that allowed for rigorous control of the interaction force (Amrein et al., 1995) and generally provided an increased resolution as compared to a conventional SFM. We also used a conventional SFM that allowed for the investigation of large sample areas and very accurate, calibrated height measurements. For the SFM studies, the films were adjusted to various film pressures on a surface balance and transferred onto a solid mica substrate by the Langmuir-Blodgett (LB) technique. The success of the LB transfer was checked by fluorescence light microscopy before and after the transfer.

EXPERIMENTAL PROCEDURES

Materials

1,2-Dipalmitoyl-sn-glycero-3-phosphocholine (DPPC) and 1,2-dipalmitoyl-sn-glycero-3-(phospho-rac-(1-glycerol)) (DPPG) were purchased from Avanti Polar Lipids (Alabaster, AL) and used without further purification. 1-Palmitoyl-2(6-((7-nitro-2-1,3-benzoxadiazo-4-yl)amino)caproyl)-sn-glycero-3-phosphocholine (NBD-PC) was obtained from Molecular Probes (Eugene, OR). All solvents were HPLC grade and were bought from Merck (Darmstadt, Germany).

Human recombinant SP-C_{pp} was a generous gift from Byk-Gulden Pharmaceuticals (Konstanz, Germany) (Schilling et al., 1987). The 34-amino acid protein contains two palmitoylated cysteines in positions 4 and 5 (Maier et al., 1992). Tricine-SDS-PAGE of the dipalmitoylated protein under nonreducing conditions yielded one band at about 5 kDa (Maier, 1995). Exact molecular weight determination was obtained by plasma desorption mass spectrometry, revealing a single, homogenous molecular ion for SP-C, corresponding to the calculated mass of 4025 Da (Maier et al., 1992).

Film balance measurements

The films were prepared on a Wilhelmy balance (Riegler and Kirstein, Mainz, Germany) with an operational area of 144 cm^2. All surface pressure-molecular area measurements were performed at 20 $\pm$ 1°C on a pure water subphase (Milli-Q_{185}Plus, Millipore GmbH, Eschborn, Germany). The film composition was DPPC:DPPG (4:1 molar ratio) and SP-C (0.4 mol %). Monolayers were formed by spreading aliquots of lipid/SP-C_{pp} mixtures directly from a $CHCl_3/CH_3OH$ (1:1, v/v) solution onto the surface. After the solvent was allowed to evaporate for 10 min, the compression was started at a rate of 3 $Å^2$/(molecule/min).

Film deposition

For Langmuir-Blodgett transfer, the films were prepared on a Lauda trough (Lauda-Königshofen, Germany) under the conditions described above. A fluorescence marker (NBD-PC, 1 mol % of lipid) was added to the SP-Cpp lipid solution before spreading. The films were equilibrated to a well-defined pressure ($\pm$1 mN/m). Freshly cleaved mica sheets (Electron Microscopy Science, Munich, Germany) were plunged through the surface at high speed (300 mm/min). The films were deposited on the upstroke (2 mm/min). Simultaneously, the compressing bar was moved at such a rate that the surface pressure remained constant. To achieve this, films at Π = 30 mN/m were transferred by adjusting the film pressure. For the films at Π = 50 mN/m (plateau region), the velocity of the compressing barrier was correlated with the deposition speed. Only samples exhibiting at least 95% transfer were considered. In addition, the deposition was checked by fluorescence light microscopy (Olympus STM5-MJS light microscope; Olympus, Hamburg, Germany). Films exhibiting a similar pattern before and after the transfer were used in this study. To check the influence of the NBD-PC on the film structure, we investigated films without the fluorescence dye. Both the surface pressure-molecular area diagrams as well as the SFM images were similar to the films that contained the dye.

SFM measurements

The samples were placed on the membrane of a modified electret microphone capsule (MCE-2500; Monacor), which acted as the force sensor in an otherwise conventional scanning tunneling microscope (STMM1 Omicron Vakuumphysik GmbH, Taunusstein, Germany). The tip was vibrated at an amplitude (A_{tip}) of 0.1–0.2 nm. The amplitude of the induced vibration of the electret membrane (A_{mem}) was then acquired as a measure of the locally variant force gradient between the tip and the microphone membrane. A_{mem} of the electret membrane was kept constant by feedback; i.e., the tip followed a surface of constant force gradient. A_{mem} was typically set within a range from 0.01 nm to 0.05 nm, which corresponded to an interaction force in the range of a few nanonewtons.

A conventional SFM was used (Park Scientific Instrument, Autoprobe cp) in the contact mode (i.e., with the tip in contact with the sample) using silicon cantilevers (type F14, spring constant $\approx$ 0.1 N/m; nanosensors GmbH, Aidlingen-Dachtel, Germany) as the probe. The interaction force was dominated by strong adhesion and usually amounted to more than 10 nN.

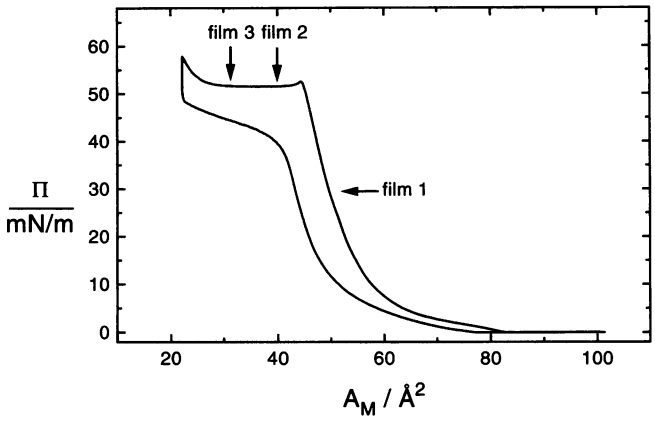

FIGURE 1 Surface pressure, depending on the mean molecular area for a mixed phospholipid (DPPC:DPPG, 4:1 molar ratio) and SP-C (0.4 mol %) film. The pressure-area diagram shows a prominent plateau. Here matter is removed from the monolayer. The back trace of the compression curve proves that this process is fully reversible. In the diagram, the conditions are noted where the different films used for SFM were transferred. Note that film 1 was transferred below the plateau region, whereas films 2 and 3 are at different stages of compression in the plateau.

RESULTS AND DISCUSSION

Films of DPPC, DPPG, and SP-C_{pp} were transferred onto the solid mica support at a film pressure of 30 mN/m (49 Å^2 molecular area, film 1), 53 mN/m (39 Å^2 molecular area, film 2), and 53 mN/m (31 Å^2 molecular area, film 3). The pressure-area diagram (Fig. 1) shows that the first of these films was transferred below the high-compressibility region (plateau), ascribed to the exclusion of matter from the monolayer. Films 2 and 3 were a series of increasing exclusion in the plateau region. In Fig. 2, fluorescence microscopy images are shown of a film (π = 53 mN/m; film 3) before and after the LB transfer. The characteristic appearance of dark domains embedded in a bright background was not disrupted by the transfer. Using fluorescence-labeled SP-Cpp instead of NBD-PC, similar fluorescence microscopical images were obtained (von Nahmen et al., manuscript submitted for publication). Therefore, the bright area was identified as being enriched in protein. Films containing only DPPC, DPPG, and NBD-PC showed no structural similarity to the film structures presented below.

SFM images of the LB films at a pressure of 30 mN/m

The SFM images of films transferred at a pressure of 30 mN/m exhibited smooth, polygonal patches separated by a corrugated interspace. The level patches had a diameter of several micrometers and covered most of the sample area. Their size and shape were quite variable. On the basis of comparisons with fluorescence microscopy (von Nahmen et al., manuscript submitted for publication), the level areas were the phase consisting mainly of lipid. The ruffled regions consisted of highly concentrated protein. This also became evident from the fact that when a film had a higher proportion of SP-Cpp, a larger fraction of the area was corrugated (results not shown; Pèrez-Gil et al., 1992a). The peak height of the film was the same for all of the topologically different areas.

Fig. 3 shows a SFM image of the border region of a lipid patch (*top left*) toward the corrugated interspace (*lower part* of Fig. 3). Toward the lipidic phase, there are intercepted fissures in an open spiral form. They turn more often and form smaller structures toward the region rich in protein. Finally, the fissures enclose polygons or spirals. Interestingly, these polygons have a shape that resembles the shape

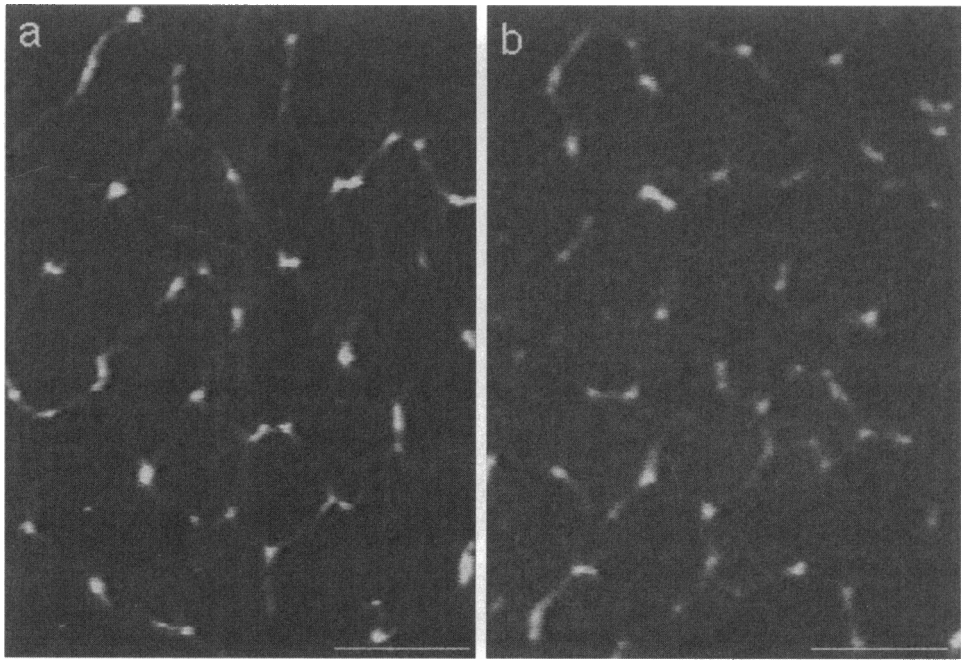

FIGURE 2 Fluorescence light micrographs of the mixed film before (*a*) and after (*b*) the Langmuir-Blodgett transfer of film 3 (bar = 25 μm). Bright areas are due to the fluorescence dye NBD-PC. It has been shown (Nahmen et al., manuscript submitted for publication) that this dye is always found in the same phase as the SP-C. Hence there are polygonal lipid patches that are surrounded by a protein-rich rim. This arrangement was not disrupted by the Langmuir-Blodgett transfer and was seen in the SFM of the transferred films (see below).

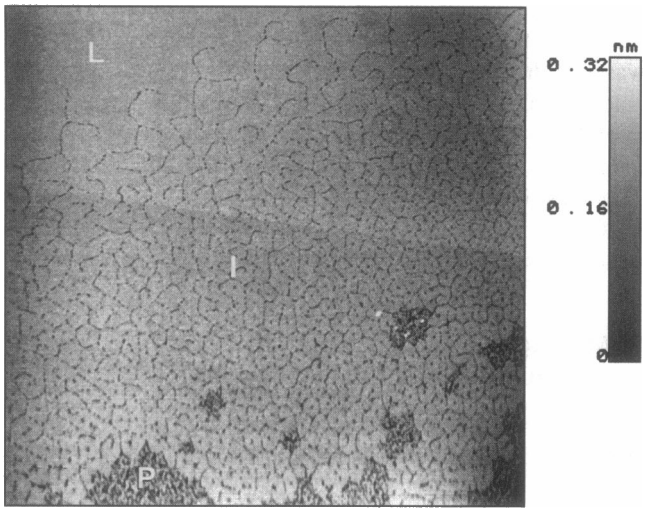

FIGURE 3 SFM topography of a film that was transferred below the plateau region of the pressure-area diagram (film 1). The image shows the border of a lipid patch facing toward the protein-rich interspace. There are three distinct regions: a smooth area that is assumed to contain only lipids (denoted by L), an intermediate area (I), and a region of a network rich in protein (P). The picture is 2.8 μm $\times$ 2.5 μm.

of the whole lipid patches, although they are one to two orders of magnitude smaller in diameter.

The protein-rich interspace was covered, not only by these small polygons, but also by regions that gave the impression of a network of filaments (e.g., *bottom right* of Fig. 3, denoted by P; Fig. 4 *a*, denoted by P). The network sometimes appeared as a dense array of filaments lying on the surface (Fig. 4 *b*, denoted by *arrows*). These arrays could be composed of long helical strands (Fig. 4 *b*). Surface balance studies on small hydrophobic α-helical polypeptides, similar to the hydrophobic moiety of the SP-C, revealed that they adopt a higher order helical structure at the surface pressures considered in the present study (Lavigne et al., 1992). Such films were also shown to become ordered upon compression (Malcolm, 1973). SP-Cpp in monolayer films has been shown to be, in fact, mainly α-helical ($\sim$ 60%), with its helical axis oriented nearly parallel to the air-water interface (Creuwels et al., 1993).

The monolayer topography provides evidence of an intermediate area of mixed lipid and protein (Fig. 3, 4). The filaments that consisted presumably of protein appeared to penetrate the lipid phase; they became less dense as the interspace filled up, and the filamenteous structures were not evident deep within the lipid area (Fig. 4, *a* and *b*, *insets*). Mixed regions of lipid and protein have already been predicted on the basis of film balance studies; In 1971, Hooks (Malcolm, 1973, and references therein) observed that the pressure-area diagram of a phospholipid/α-helical polypeptide mixed film could not be accounted for by the addition of the diagrams of the pure components. This phenomenon, which is called nonideal mixing, has also been observed for the film investigated in this study (Taneva and Keough, 1994c). Hooks concluded that the lipids would not penetrate the "polymer micelles" (filaments). He found that the two are immiscible, with "some lipid filling in regions of bad fit between polymer micelles." This seems to exactly explain what we observed with the SFM.

It is worth noting here that in a SFM, the uppermost level of a structure is usually measured correctly. On the other hand, the finite size of the tip may prevent narrow indentations from being probed to the bottom. For the same reason, elevations usually appear broadened. Hence, in Figs. 3 and 4, the depth of the fissures in the corrugated areas may be an

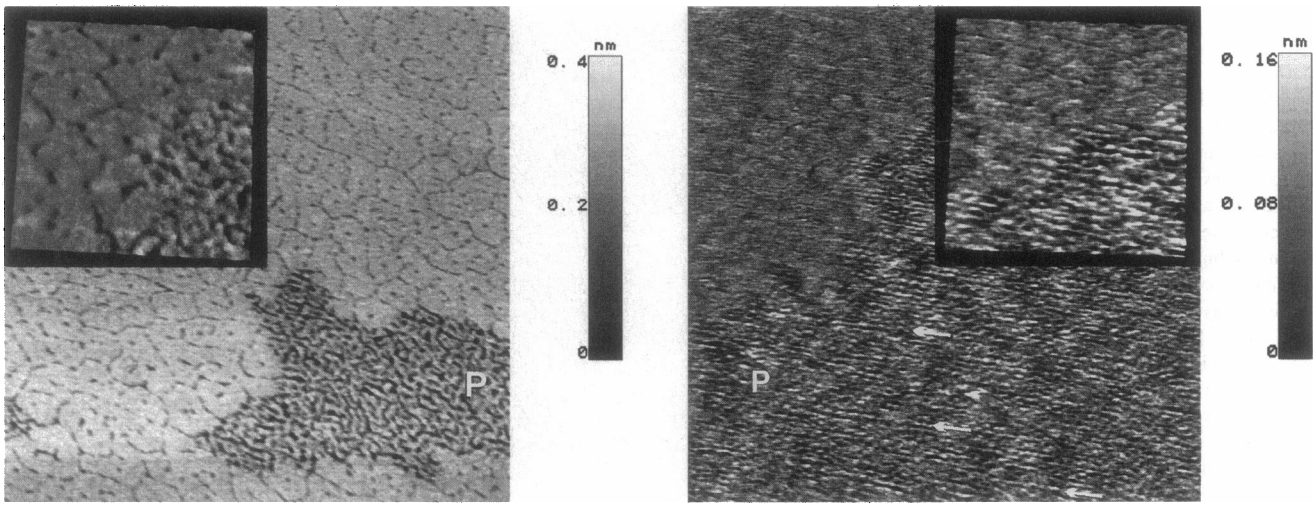

FIGURE 4 SFM topography of film 1. The protein-rich areas occasionally consisted of a disordered network (*a*, denoted by P), as well as ordered arrays of filaments (*b*, three individual filaments are denoted by *arrows*). Note that for both types of arrangements, the filamenteous structure is weakly visible in the dense intermediate regions. Both pictures are 1 μm $\times$ 1 μm. The insets are higher magnification images (1.5 times) in pseudo-three-dimensional display.

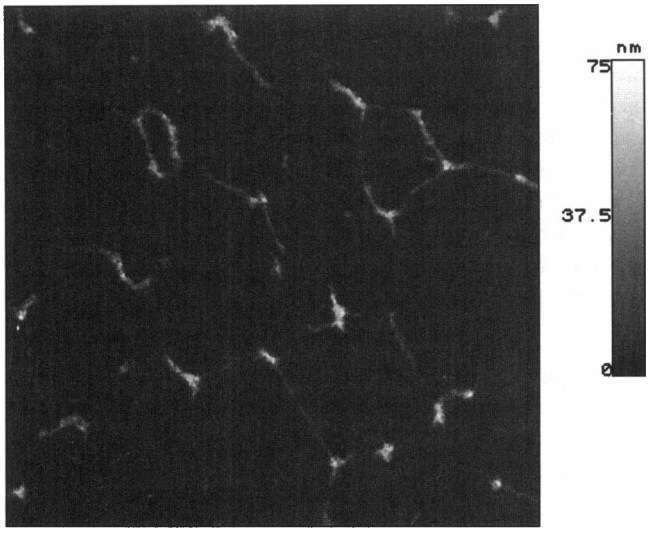

FIGURE 5 Low-magnification SFM topography of a film transferred in the plateau of the pressure-area diagram (film 3). The lipid patches are now surrounded by a rim of planar protrusions. They arose in the area, whereas in the less compressed film there was a corrugated interspace (Figs. 3 and 4). The protrusions occur as integer multiples of 55–65 Å. The picture is 65 μm × 60 μm.

underestimate and the width of the filamenteous structures an overestimate.

SFM images of the LB films in the plateau region

Fig. 5 represents a low-resolution SFM image of a film (film 3) that was transferred in the plateau region of the pressure-area diagram. The image shows large, flat, polygonal patches surrounded by a rim of protrusions. The polygonal patches were identified as the pure lipid phase. This becomes evident from comparison with the FLM images of the LB films transferred at the respective surface pressures (Fig. 2). Higher resolution SFM images of the rim that surrounded the lipid patches revealed planar protrusions. They often occurred in multiple layers. In a natural system (rabbit lung) such multilayer structures were in fact observed as well (Schürch et al., 1995).

The location of the protrusions became more confined and the number of layers increased with increasing compression of the film before the LB transfer (Fig. 6). The overall shape of the protrusions suggests that upon compression many small, round patches were squeezed out of the monolayer. They then may have grown in size and coalesced to form the larger structures. In Fig. 7 the fine structure of the film can be seen on the different layers in a pseudo-three-dimensional view (although it was less well resolved than the monolayer). A similar fine topographical structure is seen on the different steps, as in the intermediate and filamenteous area of film 1 (Figs. 3 and 4). This indicates that these regions have mediated the formation of the planar exclusion structures.

The protrusions seen in the SFM arose in the regions that appeared bright in the FLM and, hence, contained the NBD-PC in high concentration. It is assumed that the lipids with the bulky NBD groups are found in the regions of higher fluidity and lower packing density. For the same reason, the proteins may also be enriched in this phase. This assumption was verified by using fluorescence-labeled SP-C instead of NBD-PC. In this case too, a high fluorescence intensity was found in the region where the protrusions arose.

The height of a single step within the region of the planar protrusions varied between 55 and 65 Å. This is slightly larger than the height of a DPPC double layer in the gel phase, as measured with the SFM under similar conditions (~50 Å, data not shown). For more reasons than height

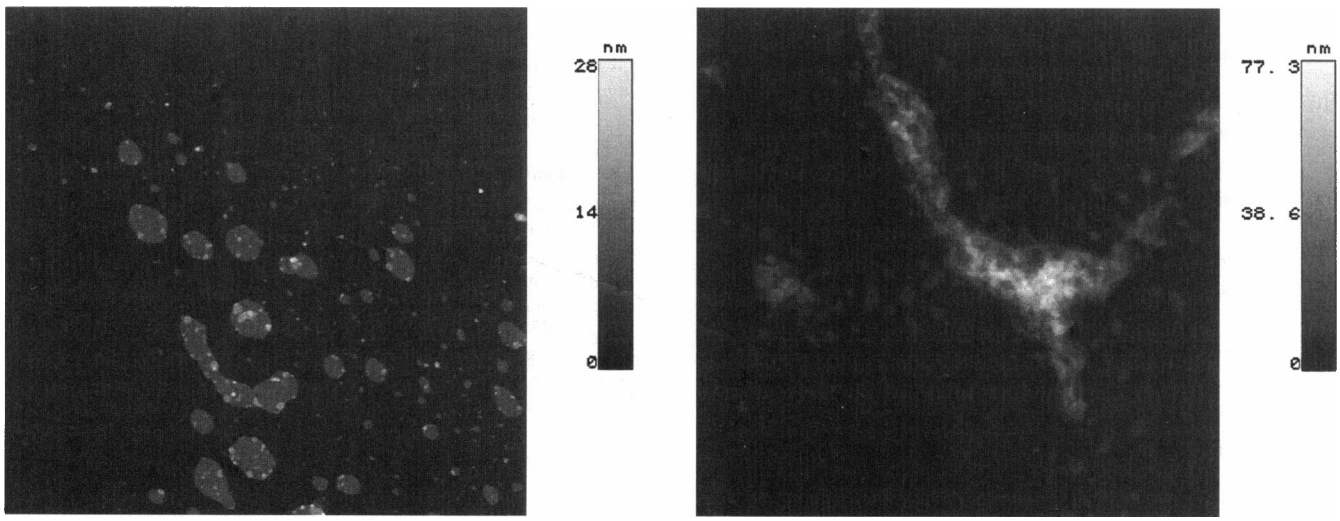

FIGURE 6 Higher magnification topographies of films, transferred at different compressions. (*Left*) Region of protrusions of a film that was transferred just at the onset of the plateau of the pressure-area diagram (film 2). (*Right*) A film (film 3) that was more compressed. Note that the area of protrusions became more confined and the number of steps increased upon compression. Both pictures are 10 μm × 9.5 μm.

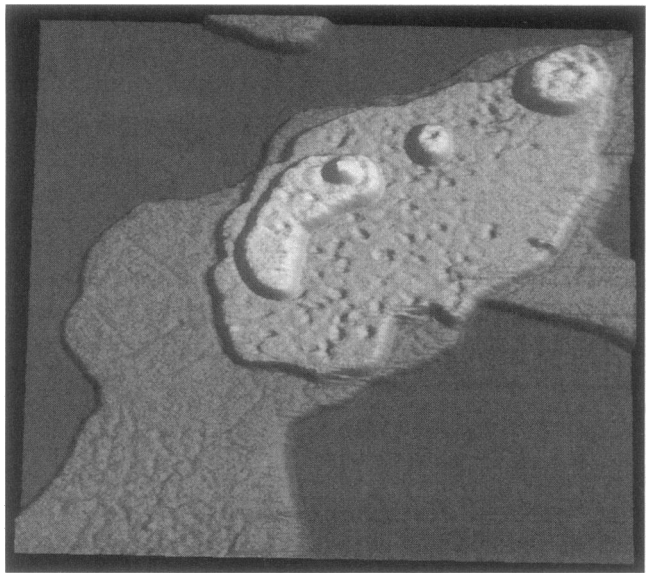

FIGURE 7 Pseudo-three-dimensional view of some protrusions. Note that a similar fine topographical structure is seen on the different steps as in the intermediate and filamenteous area of film 1, although it is less well resolved. This indicates that these regions have mediated the formation of the planar exclusion structures. Each single step is about 6 nm high. The picture is 1.2 μm $\times$ 1 μm.

measurement alone, we concluded that the protrusions were based on integer multiples of a double layer. When the film was compressed within the plateau region of the pressure-area diagram, any reduction of the monolayer area was found to produce further protrusions. The areas of all layers of the protrusions summed up to half of the area expelled from the monolayer in the plateau (e.g., the area of film 3 was reduced by 31% within the plateau region of the pressure area diagram. The corresponding sum of the areas of all layers of the protrusions was 15%, calculated from a SFM image of 60 μm $\times$ 60 μm.).

CONCLUSIONS

The model system investigated shared principal biophysical properties with natural pulmonary surfactant, even though it contained only three out of many compounds found in the natural system. The spread monolayer showed a plateau above Π = 50 mN/m, where some of its matter was reversibly removed from the monolayer. Within this plateau, the covered area of the interface could be reduced and expanded by a factor of almost 2, without a significant change in the surface tension. The surface tension was further reduced upon reduction of the area beyond the plateau. It has been suggested that, upon expiration, the more fluid components for the surfactant are being constantly removed from the monolayer. Upon inspiration, new material could then adsorb to the monolayer from vesicles each time the equilibrium surface tension is exceeded. The present study demonstrates that, in the model system used, the material removed from the monolayer remained associated with it. On expansion, it respreads into the monolayer, ensuring a closed coverage of the surface. The SFM unveiled a specific protein-lipid complex structure in the monolayer that has mediated a reversible formation of lamellar protrusions upon compression. The protrusions were, in principle, based on lipid double layers, although they were slightly thicker through the content of the SP-Cpp. In the natural system this mechanism may be responsible for keeping the surface tension of the surfactant constantly low over the range of area encountered upon breathing.

We thank R. Reichelt and H.-J. Galla for very valuable discussions and continued support and L. Melanson for careful English corrections.

This work was supported by grants Re 782/2-1 from the Deutsche Forschungsgemeinschaft, IV A 6-400 005 91 from the Ministerium für Wissenschaft und Forschung des Landes Nordrhein-Westfalen, and BEO 310855 from the Ministery of Science and Technology (BMBF).

REFERENCES

Amrein, M., M. Schenk, A. von Nahmen, M. Sieber, and R. Reichelt. 1995. A novel force-sensing arrangement for combined scanning force/scanning tunnelling microscopy applied to biological objects. *J. Microsc.* 179:261–265.

Bangham, A. D., C. J. Morley, and M. C. Phillips. 1979. The physical properties of an effective lung surfactant. *Biochim. Biophys. Acta.* 573: 552–556.

Brown, E. S. 1964. Isolation and assay of dipalmitoyl lecithin in lung extracts. *Am. J. Physiol.* 207:402–406.

Clements, J. A., E. S. Brown, and R. P. Johnson. 1958. Pulmonary surface tension and the mucous lining of the lungs: some theoretical considerations. *J. Appl. Physiol.* 12:262–268.

Creuwels, L. A. J., R. A. Demel, L. M. G. van Golde, B. J. Benson, and H. P. Haagsman. 1993. Effect of acylation on structure and function of surfactant protein C at the air-liquid interface. *J. Biol. Chem.* 268: 26752–26758.

Curstedt, T., J. Johansson, P. Persson, A. Eklund, B. Robertson, B. Löwenadler, and H. Jörnvall. 1990. *Proc. Natl. Acad. Sci. USA.* 87: 2985–2989.

Enhorning, G. 1977. A pulsating bubble technique for evaluating pulmonary surfactant. *J. Appl. Physiol.* 43:198–203.

Goerke, J., and J. A. Clements. 1986. Alveolar surface tension and lung surfactant. *In* Handbook of Physiology, Section 3: The Respiratory System, Vol. III, Part 1. A. P. Fishman et al., editors. American Physiological Society, Bethesda, MD. 247–261.

Harwood, J. L. 1987. Lung surfactant. *Prog. Lipid Res.* 26:211–256.

Hawgood, S. 1989. Pulmonary surfactant apoproteins: a review of protein and genomic structure. *Am. J. Physiol.* 1:13–22.

Johansson, J., T. Curstedt, and B. Robertson. 1994a. The proteins of the surfactant system. *Eur. Respir. J.* 7:372–391.

Johansson, J., T. Szyperski, T. Curstedt, and K. Wüthrich. 1994b. The NMR structure of the pulmonary surfactant-associated polypeptide SP-C in an apolar solvent contains a valyl-rich α-helix. *Biochemistry.* 33: 6015–6023.

Lavigne, P., P. Tancrède, F. Lamarche, and J.-J. Max. 1992. Packing of hydrophobic α-helices: a study at the air/water interface. *Langmuir.* 8:1988–1993.

Maier, C. 1995. Isolierung, Strukturaufklärung und chemische Modifizierung von natürlichen und gentechnisch hergestellten SP-C-Proteinen des Lungensurfactantsystems. Hartung-Gorre Verlag, Konstanz. 108–120.

Maier, C., K. Baumeister, K. Hägele, E. Bauer, E. Hannappel, R. Nave, E. Sturm, U. Krüger, K. P. Schäfer, and M. Przybylski. 1992. Primary structure elucidation, microheterogeneity and surfactant function of natural and recombinant lung surfactant lipoproteins. *In* Peptides 1992

(Proc. 22nd Eur. Peptide Symp.). C. H. Schneider and A. N. Eberle, editors. Escom Science Publishers.

Malcolm, B. R. 1973. The structure and properties of monolayers of synthetic polypeptides at the air-water interface. *Prog. Surf. Membr. Sci.* 7:183–229.

Notter, R. H., S. A. Tabak, and R. D. Mavis. 1980. Surface properties of binary mixtures of some pulmonary surfactant components. *J. Lipid Res.* 21:10–22.

Oosterlaken-Dijksterhuis, M. A., H. P. Haagsman, L. M. G. van Golde, and R. A. Demel. 1991a. Characterisation of lipid insertion into monomolecular layers mediated by lung surfactant proteins SP-B and SP-C. *Biochemistry.* 30:10965–10971.

Oosterlaken-Dijksterhuis, M. A., H. P. Haagsman, L. M. G. van Golde, and R. A. Demel. 1991b. Interaction of lipid vesicles with monomolecular layers containing lung surfactant proteins SP-B or SP-C. *Biochemistry.* 30:8276–8281.

Pattle, R. E. 1958. Properties, function and origin of the alveolar lining layer. *Proc. R. Soc. Lond.* 148:217–240.

Pèrez-Gil, J., K. Nag, S. Taneva, and K. M. W. Keough. 1992a. Pulmonary surfactant protein SP-C causes packing rearrangements of dipalmitoylphosphatidylcholine in spread monolayers. *Biophys. J.* 63:197–204.

Pèrez-Gil, J., J. Tucker, and G. Simatos. 1992b. Interfacial adsorption of simple lipid mixtures combined with hydrophobic surfactant protein from pig lung. *Biochem. Cell Biol.* 70:332–338.

Possmayer, F. 1988. A proposed nomenclature for pulmonary surfactant-associated proteins. *Am. Rev. Respir. Dis* 138:990–989.

Post, A., A. von Nahmen, M. Schmitt, J. Ruths, H. Riegler, M. Sieber, and H.-J. Galla. 1995. Pulmonary surfactant protein C containing lipid films at the air-water interface as a model for the surface of lung alveoli. *Mol. Membr. Biol.* 12:93–99.

Qanbar, R., and F. Possmayer. 1995. On the surface activity of surfactant-associated protein C (SP-C): effects of palmitoylation and pH. *Biochim. Biophys. Acta.* 1255:251–259.

Shelly, S. A., J. U. Balis, J. E. Paciga, C. G. Espinoza, and A. V. Richman. 1982. Biochemical composition of adult human lung surfactant. *Lung.* 160:195–206.

Schilling, J. W., Jr., R. T. White, and B. Cordell. Recombinant Alveolar Surfactant Protein. (Int. Cl C07K 13/00; AGIX 37/02). US Patent 4.659,805. 21 April 1987.

Schürch. S. 1982. Surface tension at low lung volumes: dependence on time and alveolar size. *Respir. Physiol.* 48:339–355.

Schürch, S., R. Qanbar, H. Bachofen, and F. Possmayer. 1995. The surface-associated surfactant reservoir in the alveolar lining. *Biol. Neonate.* 67(Suppl. 1):61–76.

Taneva, S. G., and K. M. W. Keough. 1994a. Dynamic surface properties of pulmonary surfactant proteins SP-B and SP-C and their mixtures with dipalmitoylphosphatidylcholine. *Biochemistry.* 33:14660–14670.

Taneva, S. G., and K. M. W. Keough. 1994b. Pulmonary surfactant proteins SP-B and SP-C in spread monolayers at the air-water interface. I. Monolayers of pulmonary surfactant protein SP-B and phospholipids. *Biophys. J.* 66:1137–1148.

Taneva, S. G., and K. M. W. Keough. 1994c. Pulmonary surfactant proteins SP-B and SP-C in spread monolayers at the air-water interface. II. Monolayers of pulmonary surfactant protein SP-C and phospholipids. *Biophys. J.* 66:1149–1157.

Taneva, S. G., and K. M. W. Keough. 1994d. Pulmonary surfactant proteins SP-B and SP-C in spread monolayers at the air-water interface. III. Proteins SP-B plus SP-C with phospholipids in spread monolayers. *Biophys. J* 66:1158–1166.

Tchoreloff, P., A. Gulik, B. Denizot, J. E. Proust, and F. Puisieux. 1991. A structural study of interfacial phospholipid and lung surfactant layers by transmission electron microscopy after Blodgett sampling: influence of surface pressure and temperature. *Chem. Phys. Lipids.* 59:151–165.

von Neergaard, K. 1929. Neue Auffassungen über einen Grundbegriff der Atemmechanik. Die Retraktionskraft der Lunge, abhängig von der Oberflächenspannung in den Alveolen. *Z. Gesamte Exp. Med.* 66:373–394.

Wang, Z., S. B. Hall, and R. H. Notter. 1995. Dynamic surface activity of films of lung surfactant phospholipids, hydrophobic proteins, and neutral lipids. *J. Lipid Res.* 36:1283–1293.

Weaver, T. E. 1988. Pulmonary surfactant-associated proteins. *Gen. Pharmacol.* 19:361–368.